Title	The Deep Earthquake of June 22, 1966 in Banda Sea : A Multiple Shock
Author(s)	OIKE, Kazuo
Citation	Bulletin of the Disaster Prevention Research Institute (1969), 19(2): 55-65
Issue Date	1969-11
URL	http://hdl.handle.net/2433/124770
Right	
Type	Departmental Bulletin Paper
Textversion	publisher

Bull. Disas. Prev. Res. Inst., Kyoto Univ., Vol. 19, Part 2, No. 158, Nov. 1969

The Deep Earthquake of June 22, 1966 in Banda Sea: A Multiple Shock

By Kazuo OIKE

Abstract

The body waves of the deep earthquake which occurred in the Banda Sea region on June 22, 1966, were recorded by the long-period seismographs of the WWSSN, and they showed very peculiar aspects compared with the waveforms of normal deep earthquakes. In the record of the P wave at each station two successive P phases were clearly distinguished.

The fault plane solutions of the first P phases, P_1, and the second, P_2, showed nearly the same pattern. Accordingly P_2 phase was not the stopping phase that is to be expected from the moving source.

The relation between the positions of the two foci and the difference between their origin times were determined from the distribution of the difference between the arrival times of the two P waves. The results showed that the second focus was situated on one of the nodal planes of the first shock at a distance of 22 kilometers in the direction of N170°E along the horizontal plane. The difference between the origin times was found to be about 4.8 seconds.

The superposition of the two impulsive waves synthesized from the impulse response of the crust-instrumental system and the amplitudes calculated by assuming the fault plane solutions, the relation of the focal positions and the ratio of the seismic moments of the two shocks, gave the theoretical waveform for each station. They showed very good coincidence with the observed records. The most appropriate ratio of the seismic moments was 4.0.

Comparing the amplitudes calculated from the point source of shear dislocation with the observed ones, the seismic moments of the first and second shocks were found to be about 1.4×10^{25} and 5.6×10^{25} dyne·cm, respectively.

1. Introduction

Much useful information for the study of focal mechanism has been obtained by investigations of the time series of earthquakes which have occurred in restricted regions. Especially in the case of shallow earthquakes the characteristics of the fore-shocks, after-shocks, and earthquake swarms have been researched in regard to the nature of the crust. The main purpose of these studies is to clarify the general characteristics of the mechanism of occurrence of the earthquakes by the statistical analysis of the seismic activities.

On the other hand, some examples of earthquakes which took place successively within short time intervals for instance a few seconds, in the same region, were presented and investigated in detail by Miyamura et al[1]. Such earthquakes are called multiple shocks. This problem of multiple shocks is significant as regards the establishment of the perfect model of earthquake origins because of its relation to the strain release and the focal mechanism.

But multiple shocks, if many exist, usually seem to be one shock and it is very difficult to find them. On the other hand, in the case of micro-earthquakes or smaller first shocks than second shocks, the seismic waves recorded at a station which is very near the epicenter are instantly decreased and the phases of each shock are clearly identified, and so it is easy to discover multiple shocks. Two examples of the multiple shocks of micro-earthquakes are shown in Fig. 1. In them two shocks whose waveforms were the same from beginning to end took place successively within a time interval of 14.2 seconds for the upper couple and about 13 minutes for the lower. The coincidence of the waveforms of such short periods means that the foci of the two shocks are exactly the same or contiguous. Thus micro-earthquakes can be used to investigate the features of multiple shocks, because many examples seem to be observed.

Several shallow earthquakes of large magnitude, for example the Niigata earthquake of June 16, 1964, have been studied from the view point of determining whether they were multiple shocks or not[1]. But the second and the third P phases after the initial P waves of the records of the Niigata earthquake were interpreted as the pP and the stopping phases respectively by Hirasawa[2], and it is difficult to decide whether this earthquake was a multiple shock or not, only from seeing the various records of the P waves. Wyss and Brune analysed the seismograms of the Alaska earthquake of March 28, 1964, and showed the rupture propagated in various azimuthal directions with the average propagation velocity of 3.5 km/sec.[3] Wu showed that the main shock of the Parkfield earthquake of June 28, 1966 could be represented by a series of shocks separated in space and time.[4] Although such results have been obtained, it is generally hard to find multiple shocks of shallow focus and large magnitude, for many reflected or converted waves are recorded successively after the direct body waves.

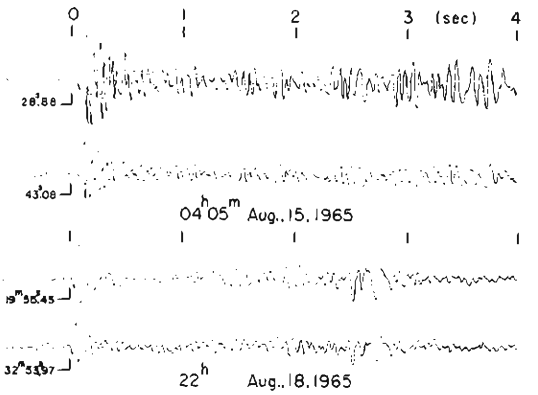

Fig. 1. Two examples of multiple shocks of micro-earthquakes.

On the occasion of deep earthquakes, the simple waveforms are usually seen in the records and no later phases just after the initial P waves are seen. Mikumo analysed the long-period P waves of four intermediate earthquakes, and showed that the time functions of the observed P waves were in good accordance with the theoretical ones calculated from the point source of the shear dislocation[5]. For this reason it must be comparativey easy to detect multiple shocks of deep focus if they exist. But deep earthquakes are not generally accompanied even by after-shocks, and they occur in most cases in isolation. In addition to this there are differences between the constitution and the physical conditions of the crust and the mantle. Therefore the mechanism of shallow earthquakes and deep ones must be different. Thus it is very important for studying this problem to

know whether there are any multiple shocks in deep earthquakes or not.

It is the purpose of this paper to explain that the deep earthquake of June 22, 1966, which occurred in the Banda Sea area and was 507 kilometers deep was a multiple shock. The results of the analyses of the fault plane solutions, the travel times and the long-period P waveforms have shown that this earthquake is a kind of multiple shock in which two shocks occurred successively within a short time interval of about 5 seconds.

2. Observational Data

The data of the origin of the earthquake which was investigated in this paper were reported by the U. S. Coast and Geodetic Survey in the Earthquake Data Report and are as follows,

origin time : June 22, 1966, $20^h\ 29^m\ 03^s.6$ (G.M.T.),
location : 7°.20S, 124°.59E (Banda Sea),
depth : 507 km, and
magnitude : 6.1 (7 stations).

The long-period P waves observed by the Z-component long-perod seismographs of the WWSSN were classified into four types considering their waveforms. Each observed P wave at almost all the stations belonged to one of the four groups of waveform types as shown in Fig. 2. The long-period P waves of deep shocks whose magnitude is about 6 usually seem to be the time function of the impulse response of the crust-instrumental system. The four types of waveforms shown in Fig. 2 can be composed by the superposition of two such impulse responses giving about 5 seconds time delay from the first pulse to the second. The A type wave is synthesized from two pulses of the upward motions with nearly the same amplitudes, the B type from those of the opposite polarities and nearly the same amplitudes, the C type from those of the downward motions with comparative amplitudes and the D type from the first pulse of the small downward motion and the second pulse of the large motion with the same polarity.

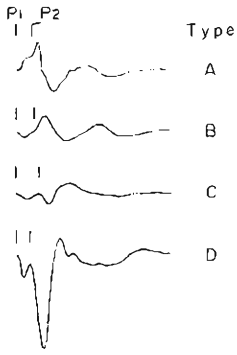

Fig. 2. Four typical P waveforms of the deep earthquake of June, 22, 1966, recorded by the Z-component long-period seismographs of the WWSSN.

From the nature of the P waves it can be presumed that these P waves contain two P phases radiating independently from two origins whose locations and depths are nearly the same, or that this earthquake is a kind of multiple shocks.

This property can be seen in the records of the short-period seismographs with high sensitivity of the micre-earthquake observation networks. Three examples of their Z-component records are shown in Fig. 3, in which the Mikazuki and Hikami stations belong to the Tottori Micro-Earthquake Observation Network and Arida belongs to the Wakayama Network. In each record the waveforms of the second phase with a large amplitude, P_2, are produced by giving the time delay of 5.5 seconds to the first phase, P_1, and multiplying the amplitude of P_1 by -3.0.

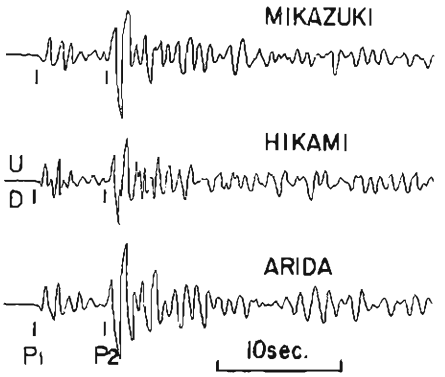

Fig. 3. The Z-component seismograms of P waves recorded by the short-period velocity seismographs at the micro-earthquake observation stations.

The data read from the Z-components of the long-period seismographs of the WWSSN are shown in Table 1, where P_1 and P_2 mean the first and the second P phases, t_{p1} and t_{p2} are the arrival times of P_1 and P_2, and τ means the time difference between them ($t_{p2}-t_{p1}$), respectively. In Table 1, the stations are arranged in order of increasing azimuth for each polarity of P_1, and the types of waveforms written in the last column show that the P waveforms of this earthquakes partly depend upon the azimuth of the seismic wave radiation from the focus.

The value of t_{p1} were copied from the Earthquake Data Report, adding the readings of the stations without

Table 1. The P wave data. Type corresponds to the classification in Fig. 2.

Station Code	Azimuth (deg.)	Δ (deg.)	t_{P1} m	t_{P1} s	Polarity P_1	Polarity P_2	τ (sec.)	Type
DAV	4.0	14.2	32	08.2	+	+	6.7	A
KOD	289.8	50.0	37	14.0	+	(+)	5.0	(A)
POO	297.9	56.2	37	58.0	+	+	(5.5)	A
CHG	316.1	36.2	35	27.5	+	+	4.5	A
MAT	15.5	45.4	36	36.6	−	+	5.5	B
COL	25.3	95.5	41	32.3	−	−	6.7	C
RAB	85.3	27.6	34	10.0	−	+	(4.5)	C
HNR	96.2	35.0	35	14.0	−	−	5.7	C
AFI	101.9	62.8	38	40.0	−	−	5.2	C
RAR	110.0	74.1	39	49.0	−	−	(5.5)	C
CTA	123.5	24.6	33	44.0	−	−	3.7	D
RIV	140.8	36.1	35	24.6	−	−	2.5	D
TAU	154.3	40.8	36	02.4	−	−	3.5	D
ADE	156.8	30.6	34	36.7	−	−	2.9	D
SBA	171.4	73.8	39	48.0	−	−	4.9	D
SPA	180.0	82.8	40	34.0	−	−	3.0	D
MUN	196.5	25.9	33	55.2	−	−		C
PRE	243.8	92.6	41	22.5	−	−	5.6	C
BUL	249.4	93.1	41	25.0	−	−	5.6	C
NAI	269.0	87.6	41	01.3	−	−	6.2	C
AAE	279.5	87.0	41	00.0	−	−	5.7	C
JER	301.5	93.2	41	25.5	−	−	5.9	C
SHI	302.1	78.2	40	12.7	−	−	5.7	C
QUE	307.2	66.6	39	04.1	−	(+)	(2.5)	(B)
IST	310.4	98.9	41	49.0	−	−	5.9	C
SHL	316.9	45.6	36	40.5	−	+	6.1	B
HKC	341.1	31.1	34	41.8	−	+	6.5	B
BAG	350.4	23.8	33	37.5	−	+	5.6	B
MAN	350.9	22.1	33	21.0	−	+	6.4	B
ANP	354.8	32.4	34	50.1	−	+	6.4	B

reports. The travel times of P are plotted in regard to the epicentral distances in Fig. 4. The travel time curve of each later phase was calculated for the depth of 0.075R from the tables of Jeffreys and Bullen. Several seconds after the arrival of the initial P phases, there cannot be seen any later phases except PcP at the stations more than 80 degrees distant.

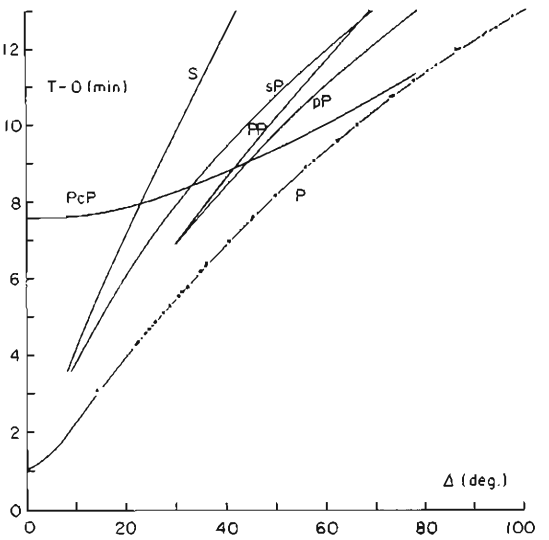

Fig. 4. The travel time curves for the focal depth of 500 km.

Some of the O-C calculated from the arrival times of P reported in the Earthquake Data Report have large values of about five seconds, which means that P_1 phases have been observed with very small amplitudes at these stations. There are also some stations from which the arrival times of P_2 have been reported in addition to that of P_1, for example MIR.

3. Fault Plane Solutions of P_1 and P_2

Figs. 5 and 6 show the fault plane solutions of P_1 and P_2. Two nodal lines for the radiation pattern of P_1 in Fig. 5 were determined to satisfy the relation between the observational amplitudes and the theoretical ones which were calculated assuming the point source of double coupled force system or shear dislocation. For four stations only the P_1 phases were read because of the saturation of the records. The minimum and maximum principal axes were determined from these fault plane solutions for P_1 and P_2, respectively. The results are shown in Table 2.

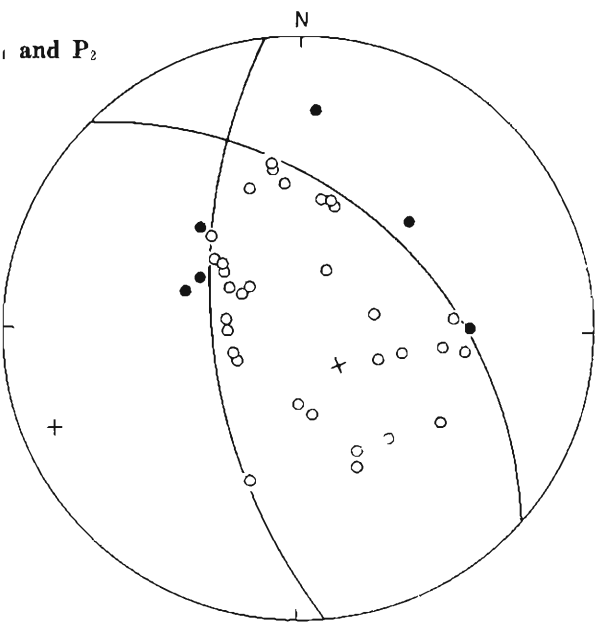

Fig. 5. The radiation pattern of P_1 waves from the first shock. The closed circles, the open circles and the crosses indicate the compressions, dilatations and the minimum and maximum principal axes, respectively.

If attention is only paid to type B in Fig. 2, the second P phases seem to be the stopping phases expected from the assumption of the moving source model which have been studied by Savage[6] or Hirasawa.[2] The stopping phases must have the opposite polarity to the initial P waves. The relation between two fault plane solutions of P_1 and P_2 shows that the P_2 waves are not the stopping phases. Therefore it is concluded that this earthquake is a multiple shock.

The directions of the minimum and maximum principal axes of the two shocks differ from each other by about 30 and 5 degrees, respectively. This seems to mean that the occurrence of the small first shock caused a slight change for the stress field around its focus. It is also supposed that the two shocks occurred because of the generation of a set of conjugate fault planes and then that the angle between these fault planes was less than 90 degrees. But this cannot all be concluded only from the present analyses of the data on hand.

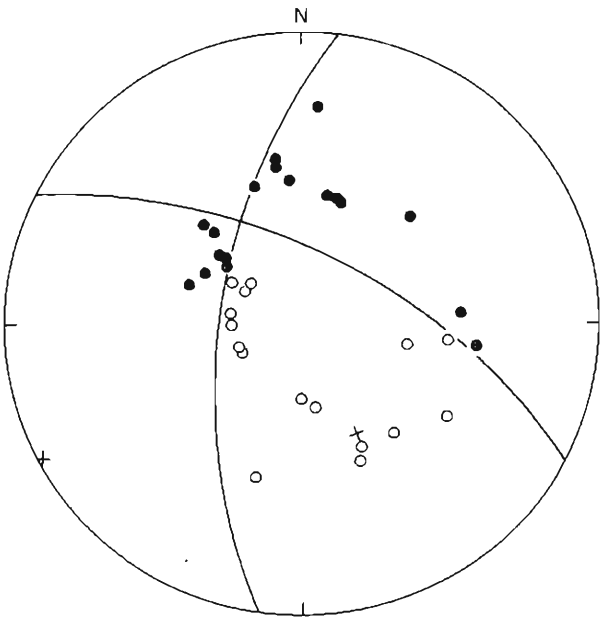

Fig. 6. The radiation pattern of P_2 waves from the second shock.

Table 2. The principal axes obtained from the fault plane solutions in Fig. 5 and 6.

	Minimum principal axis		Maximum principal axis	
	θ	φ	θ	φ
P_1	20°	144°	83°	247°
P_2	45°	151°	88°	243°

4. $P_1 \sim P_2$ Interval Times

When two P waves radiate successively from two origins, O_1 and O_2, the difference between the arrival times of the two P phases, τ_j, at the j-th station is defined as follows,

$$\tau_j = t_{02} - t_{01} - \frac{l}{v_p} \cos \delta_j \qquad (j = 1, 2, \cdots)$$

where $t_{02} - t_{01}$ is the difference between the origin times at O_1 and O_2, δ_j is the angle between $\overrightarrow{O_1O_2}$ and the direction of P_1 wave radiation for the j-th station, l is the length of $\overline{O_1O_2}$.

Using the value of τ in Table 1 the relation between τ and cos δ was investigated for various O_1O_2 directions varying its dip and azimuth angles with a 10 degree step. The most appropriate line to explain them was determined as follows,

$$\tau = 4.8 - 2.2 \cos\delta \quad \text{(sec.)}$$

They are shown in Fig. 7. The result of the direction of O_1O_2 is N170°E along the horizontal plane.

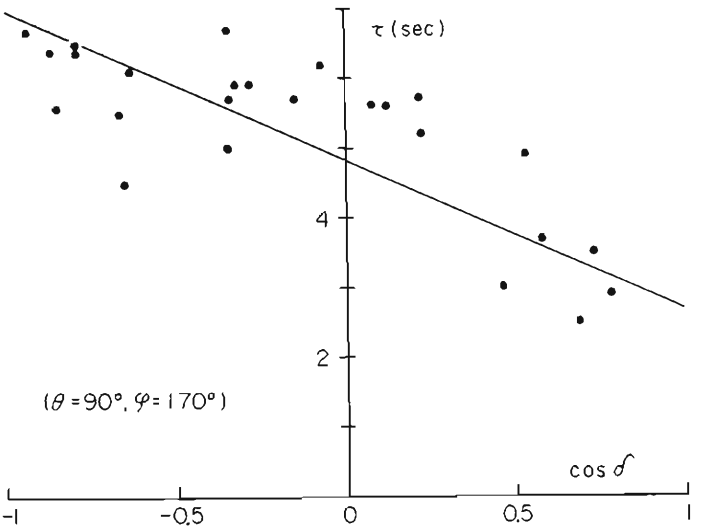

Fig. 7. The relation between the $P_1 \sim P_2$ interval times and cos δ.

The difference between the origin times of the first and second shocks is 4.8 sec. Using the value of l/v_p, the distance between O_1 and O_2, l, is determined to be 22 km. Considering this from the standpoint that there is inductivity between the earthquake origins, the propagating velocity of the infuluence is about 4.6 km/sec. This result coincides with the rupture speeds determined from the analyses of surface waves and stopping phases for several large earthquakes[2),7)].

5. Observational and Theoretical P Waveforms

The relations between the amplitudes of P_1, A_{p1}, and that of P_2, A_{p2}, which were recorded by the various types of seismographs in Japan are shown in Fig. 8. The closed circles indicate the amplitude relations of the records of the three components of the long-period seismographs at Matsushiro Observatory of J.M.A., the open circles indicate those of the ini-

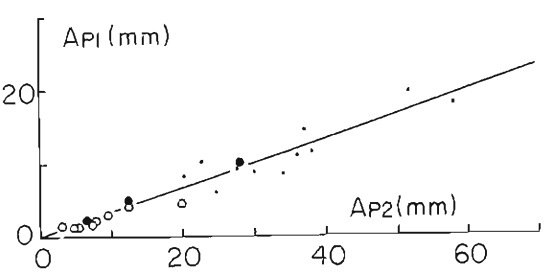

Fig. 8. The relation between the initial and the maximum amplitudes obtained by the various type seismographs in Japan.

tial motions of two phases of the short-period seismographs of the Wakayama, Shiraki and Tottori Micro-Earthquake Observation Networks, and the dots show those of their maximum amplitudes. All of them are interpreted by the relation that $A_{p2}=-3.0\ A_{p1}$, which means that the P_1 and P_2 waves observed in Japan have the same spectral structure in the wide range of frequency.

On the basis of the fact mentioned above, the theoretical P waveforms, $g_0(t)$, were calculated for each station, by superposing two pulses each of which has an adequate amplitude, polarity and arrival time, as follows,

$$g_0(t)=A\{2\lambda_1\lambda_2\cdot f_0(t)+2k\nu_1\nu_2\cdot f_0(t-\tau)\}$$

where $f_0(t)$ is the time function of the impulse response of the crust seismograph system, A is the constant related to the diminution factor and the magnification of the seismograph, k is the ratio of the seismic moments of the two shocks and λ_i and ν_i mean the direction cosines of the wave radiation angles in relation to the fault plane solutions of the two shocks, respectively. We applied one of the results of Ben-Menahem to the time function of $f_0(t)$ shown in Fig. 9. It was calculated for the continental crust and the 30-100 seismograph system of Press-Ewing type assuming an apparent velocity of 25 km/sec.[8] Although a slight systematic error will be present in the results because of applying only one time function to each station, they are not affected essentially.

The ratio of the seismic moments of the two shocks was

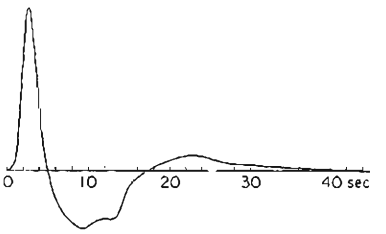

Fig. 9. The impulse response of crust-instrument system after Ben-Menahem et al. (1965).

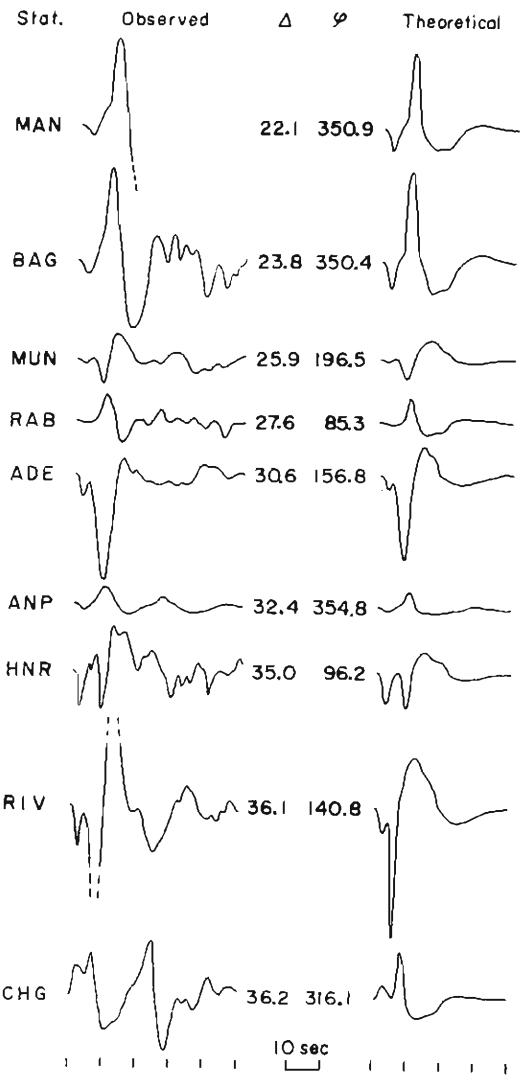

Fig. 10 (a)

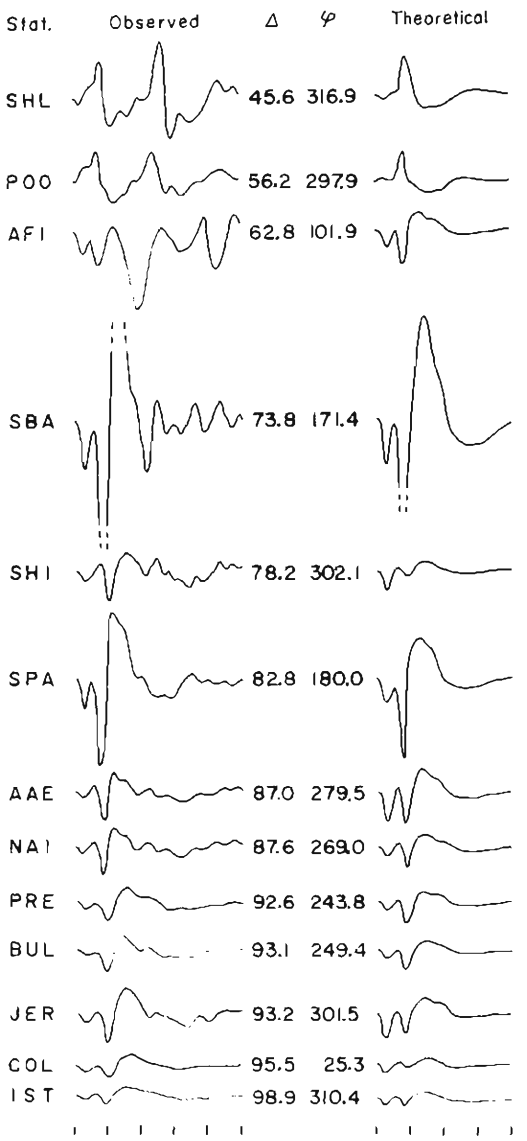

Fig. 10 (b)

Fig. 10. The comparison between the observational and the theoretical waveforms.

determined to be 4.0 to explain the observational waveforms. The calculated results of the theretical time functions are shown in Fig. 10, comparing the correspondent observational waves for each station. They are drawn up in order of increasing epicentral distance. The amplitudes of waves are arbitrary, and in Fig. 10 only the coincidence of the observational and theoretical waveforms is discussed. In the observational records at a distance of 35°-70°, the large later phases, pP and PP are found, but these later phases are not contained in the theoretical waves.

Fig. 11 shows the relation between the observational amplitudes of the initial P_1 phases and the theoretical ones. The values of the theoretical amplitudes must be multiplied by $1/2\pi\times10^{-8}$ in $(\mathrm{cm\cdot sec})^{-1}$. Assuming that this shock was caused by the shear dislocation, we can determine the seismic moment of the shock from the ratio of the amplitudes of $g_0(t)$ and the that of the observational results, $g(t)$, as follows (Mikumo),

$$\frac{|g(t)|_{max}}{|g_0(t)|_{max}} = \frac{DLW}{2\pi a}\left(\frac{b}{a}\right)^2 = \frac{M_0}{2\pi\rho a^3}$$

$$M_0=\mu DLW,$$

where D, L and W are the amplitude of dislocation, the length of the fault and its width, a and b are the velocities of the P and S waves, μ and ρ are the rigidity and the density around the focus and M_0 is the seismic moment, respectively. The results for the first and second shocks are as follows,

$$M_{01}=1.4\times10^{25},\quad M_{02}=5.6\times10^{25}\ (\mathrm{dyne\cdot cm})$$

where ρ is taken to be 4.0 g/cm.

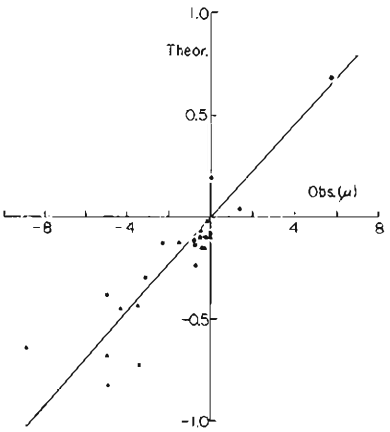

Fig. 11. The relation between the observational and the theoretical amplitudes of P_1 waves.

6. Concluding Remarks

Because the observational waves of this earthquake are sufficiently explained by the superposition of the impulsive waves from the point source model of the shear dislocation, the focus of the first shock is presumed to have a dimension of less than twenty to thirty kilometers. So it is concluded that the second shock occurred in the region just in contact with the first focus. Accordingly it is supposed that the occurrence of the first shock caused the variation of the stress field at its circumference and became the trigger for another strain release. But the problem still remains why such examples of multiple shocks have not been found among deep earthquakes.

It can be said that the propagating velocity of the influence of the generation of the first shock is 4.6 km/sec. Another problem that is left is whether the results of this propagating velocity have some significance in relation to the rupture velocity of the propagating fault or not.

Because of the resemblance of the fault plane solutions, the coincidence of the spectral structure and the results in Fig. 10, it is clear that the mechanisms of the occurrence of the two shocks are identical.

It must be attended to that the origin of the second shock determined from the arrival times of P_2 is situated on one of the nodal planes of the first shock. If deep earthquakes are caused by the shear dislocation, the fault plane of the second shock may have been generated along the extended direction of the first one or generated as a conjugate fault. Such relations between the faults can often be discovered on the earth's surface.

It is still necessary to systematically try to find more examples of deep multiple shocks. Moreover, the intermediate and shallow earthquakes must also be investigated from the viewpoint of multiple shocks. The mechanisms of earthquake occurrence must be clarified to make it possible to explain the various characteristics of the focal region containing the existence of multiple shocks.

I wish to thank Dr. Yoshimichi Kishimoto for his valuable suggestions and Dr. Takeshi Mikumo for helpful discussions about this problem. The seismograms obtained in Japan were supplied by the Matsushiro Observatory (J. M. A.) and the Wakayama, Shiraki (Tokyo Univ.) and Tottori (Kyoto Univ.) Micro-Earthquake Observation Stations. The long-period seismograms were supplied by the United States Coast and Geodetic Survey. Computations were carried out on a FACOM 230-60 computer at the Computation Center, Kyoto University.

References

1) Miyamura, S., S. Omote, R. Teisseyre and E. Vesanen: Multiple Shocks and Earthquake Series Pattern, Bull. Int. Inst. Seism. Earthq. Eng., Vol. 2, 1965,

pp. 71-92.
2) Hirasawa, T. : Source Mechanism of the Niigata Earthquake of June, 16, 1964, as Derived from Body Waves, J. Phys. Earth, Vol. 13, 1965, pp. 35-66.
3) Wyss, M and J. N. Brune : The Alaska Erathquake of 28 March 1964 : A Complex Multiple Rupture, Bull. Seism. Soc. Amer., Vol. 57, pp. 1017-1023.
4) Wu, F. T. : Parkfield Earthquake of June 28, 1966 : Magnitude and Source Mechanism, Bull. Seism. Soc. Amer., Vol. 58, 1968, pp. 689-709.
5) Mikumo, T. : Long-Period P Waveforms and the Source Mechanism of Intermediate Earthquakes, J. Phys. Earth, Vol. 17, 1969 (in preparation).
6) Savage, J. C. : The Effect of Rupture Velocity upon Seismic First Motions, Bull. Seism. Soc. Amer., Vol. 55, 1965, pp. 263-275.
7) Ben-Menahem, A. and M. H. Toksoz : Source-Mechanism from Spectra of Long-Period Seismic Surface Waves, 3, The Alaska Earthquake of July 10, 1958, Bull. Seism. Soc. Amer., Vol. 53, 1963, pp. 905-919.
8) Ben-Menahem, A., S. W. Smith and T. L. Teng : A Procedure for Source Studies from Spectums of Long-Period Seismic Body Waves, Bull. Seism. Soc. Amer., Vol. 55, 1965, pp. 203-235.